Journal of Catalysis 274 (2010) 207–214

Contents lists available at ScienceDirect

Journal of Catalysis

journal homepage: www.elsevier.com/locate/jcat

Oxygen activation sites in gold and iron catalysts supported on carbon nitride and activated carbon

Junjiang Zhu [a,*], Sónia A.C. Carabineiro [b], Dan Shan [c], Joaquim L. Faria [b], Yujun Zhu [c], José L. Figueiredo [b,**]

[a] Technical University of Berlin, Englische Str. 20, 10587 Berlin, Germany
[b] Laboratory of Catalysis and Materials (LCM), Associate Laboratory (LSRE/LCM), Department of Chemical Engineering, Faculty of Engineering, University of Porto, Rua Dr. Roberto Frias, 4200-465 Porto, Portugal
[c] School of Chemistry and Materials, Heilongjiang University, No. 74 Xuefu Road, Harbin 150080, PR China

ARTICLE INFO

Article history:
Received 2 May 2010
Revised 29 June 2010
Accepted 30 June 2010
Available online 3 August 2010

Keywords:
Oxygen activation
Carbon monoxide
Benzyl alcohol
Catalytic oxidation
Gold
Iron

ABSTRACT

The pathway of oxygen activation in oxidation reactions catalyzed either by transition metal or by gold catalysts has been extensively studied; however, this topic is still under discussion, and no consistent conclusion has been achieved up to date. One possible reason for this can be related to the fact that it is hard to find out whether the activated oxygen species come from the metal or the oxygen site. In an attempt to solve this problem, catalysts without oxygen (i.e. Fe–C_3N_4), or with controllable oxygen content (i.e. Au/AC), were tested in the oxidation of carbon monoxide in the gas phase and the oxidation of benzyl alcohol in the liquid phase. The results indicate that the metal site (i.e. Fe^{3+}, Au) alone is not able to activate molecular oxygen and that the activity of the catalyst depends intimately on the amount of oxygen-containing species (e.g. surface groups of AC) that are used for oxygen activation. As a result, a scheme for the oxidation reaction is proposed, where the metal and oxygen sites of the catalyst are accounted for the adsorption and activation of substrate and molecular oxygen, respectively.

1. Introduction

Catalytic oxidations can be classified into two types [1]: (1) complete oxidation, which is used for the abatement of various toxic compounds in catalytic purification systems, such as the oxidation of carbon monoxide (CO); (2) selective oxidation, which is used for the synthesis of desired chemical products, such as the selective oxidation of benzyl alcohol to benzaldehyde or benzoic acid.

Gold, as well as transition metals, can be used as catalysts for oxidation reactions and have been extensively investigated in the oxidation of CO [2–7], benzyl alcohol [8–11], and other intermediate products [12]. However, their reactivity toward oxygen is largely different: transition metals (e.g. Fe) readily react with molecular oxygen to form metal oxides, while gold shows strong resistance to attack by molecular oxygen.

The mechanism of oxidation reactions must include a step of oxygen activation, since in most cases molecular oxygen cannot directly oxidize the substrates (e.g. CO, CH_4) [1]. With oxide catalysts, it is generally accepted that the activation of molecular oxygen takes place on the defects or oxygen vacancies, as shown by ^{18}O isotope experiments [13–16]. However, the behavior of the metal is still not clear: could it show activity for the oxidation reaction? That is, could oxygen activation proceed also on the metal site of the catalyst (e.g. Fe^{3+} of Fe_2O_3)?

For gold catalysts, two pathways for oxygen activation were proposed in the literature: one takes place directly on the gold surface [17,18], and the other on the defects of the oxide support [6,19]. The results reported in the literature have been interpreted in different ways. For example, for CO oxidation on a Au/MgO catalyst, Schubert et al. [20] claimed that MgO is an "inert" support and that the activity depends mainly on the gold particle size, while Yan et al. [21] showed that MgO is an "active" support, as the activity is proportional to the amount of "F centers" in the oxide support. In spite of many characterization studies, no definitive conclusion has been reached up to date, although the number of articles which tend to support the view that adsorption and activation of molecular oxygen takes place on the oxide carrier (not on gold) is increasing [22–26].

Although some earlier papers of Haruta report on the activity of unsupported gold (powders with mean particle size of ~100 nm) for CO oxidation [27,28], a more recent study carried out by this group showed that the activity of the gold powder had a strong correlation with the surface concentration of Ag impurities [29]. The authors concluded that the activity of the Au powder observed could only be ascribed to the so-called contact interface effect, due to the existence of Ag, which was probably partly oxidized and present on the surface of the Au powder [29]. Bäumer's group

* Corresponding author.
** Corresponding author.
E-mail addresses: ciaczjj@gmail.com (J. Zhu), jlfig@fe.up.pt (J.L. Figueiredo).

0021-9517/$ - see front matter © 2010 Elsevier Inc. All rights reserved.
doi:10.1016/j.jcat.2010.06.018

also reported that the unexpectedly high catalytic activity of nanoporous gold foams for CO oxidation, in the temperature range of 0–50 °C, was related with the presence of residual silver [30]. Quinet et al. studied the preferential oxidation of CO in the presence of hydrogen over a silver-free-unsupported gold powder (mean particle size ~20 nm), but in this case, the initially weakly active unsupported gold powder could be activated or regenerated by the presence of H_2 in the reaction feed [31].

Surface science studies carried out on gold single crystal surfaces also showed that the rate of CO oxidation was higher when the single crystal surfaces were precovered with atomic oxygen, as highlighted in a recent review [32]. This was shown for Au(1 1 0) [33], Au(1 1 1) [34–37], and Au(2 2 1) surfaces [38]. Moreover, DFT results obtained on Au(3 2 1) surface showed that the reaction of CO oxidation by atomic oxygen occurs almost without any activation energy on a reconstructed surface, whereas a moderate barrier of 58 kJ mol^{-1} was computed for the direct reaction with molecular oxygen occurring at the surface steps [39].

More recently, Rodriguez et al. studied the interaction and dissociation of O_2 on Au nanoparticles supported on TiC(0 0 1), an oxygen-free support [40]. They found that the dissociation of O_2 at room temperature was enhanced by the presence of the TiC, in comparison with oxide supports. The results suggest that chemisorbed O_2 is the active species involved in the low temperature (<200 K) oxidation of CO, as in the case of Au/oxide supports.

The difficulty in identifying the site for oxygen activation may be due to the fact that catalysts used for oxidation reactions contain oxygen themselves. This is true not only for oxides and oxide-supported gold catalysts, but also for carbon-supported gold catalysts (Au/C), since the oxygen functional groups of the carbon support have to be accounted for [41,42]. Therefore, it is hard to find out whether oxygen is activated directly on the metal sites, or transferred from the oxygen sites (or oxygen vacancies) of the oxide supports. This might be in part the reason why different authors suggest several activated oxygen species (e.g. Au–O^{2-} [43,44] and Au–O_2^- [23,45]) on different gold catalysts, the presence of O^{2-} and O_2^- species being commonly observed in oxides [46]. Conventional techniques, such as FTIR and XPS, cannot differentiate whether the oxygen species originate from gold or from the oxide support.

Motivated by the earlier questions, a catalyst without oxygen was chosen for the present work in order to clarify these questions. A recent work by Wang et al. [47] indicates that the preparation of a metal catalyst without oxygen is possible, the matrix C_3N_4 being inert to oxygen in air at temperatures as high as 550 °C (see Fig. 1A). This offers an opportunity to try to clarify whether the metal site alone could be used for oxygen activation. On the other hand, it is known from past literature that carbon is a promising support for gold catalysts used in selective oxidation [10] and that the amount of surface oxygen functional groups of the carbon support can be controlled easily by thermal treatments under inert atmosphere (e.g. N_2) [41]. This also allows for the opportunity to investigate the relationship between activity and the oxygen content, in an attempt to clarify the role of oxygen species in the reaction. Gas phase oxidation of CO and liquid phase selective oxidation of benzyl alcohol were used as model reactions.

2. Experimental

2.1. Preparation of catalysts

Synthesis of Fe–C_3N_4 [47]: One gram dicyandiamide was mixed with 5 mL deionized water, heated and stirred at 80 °C with 0.1 g

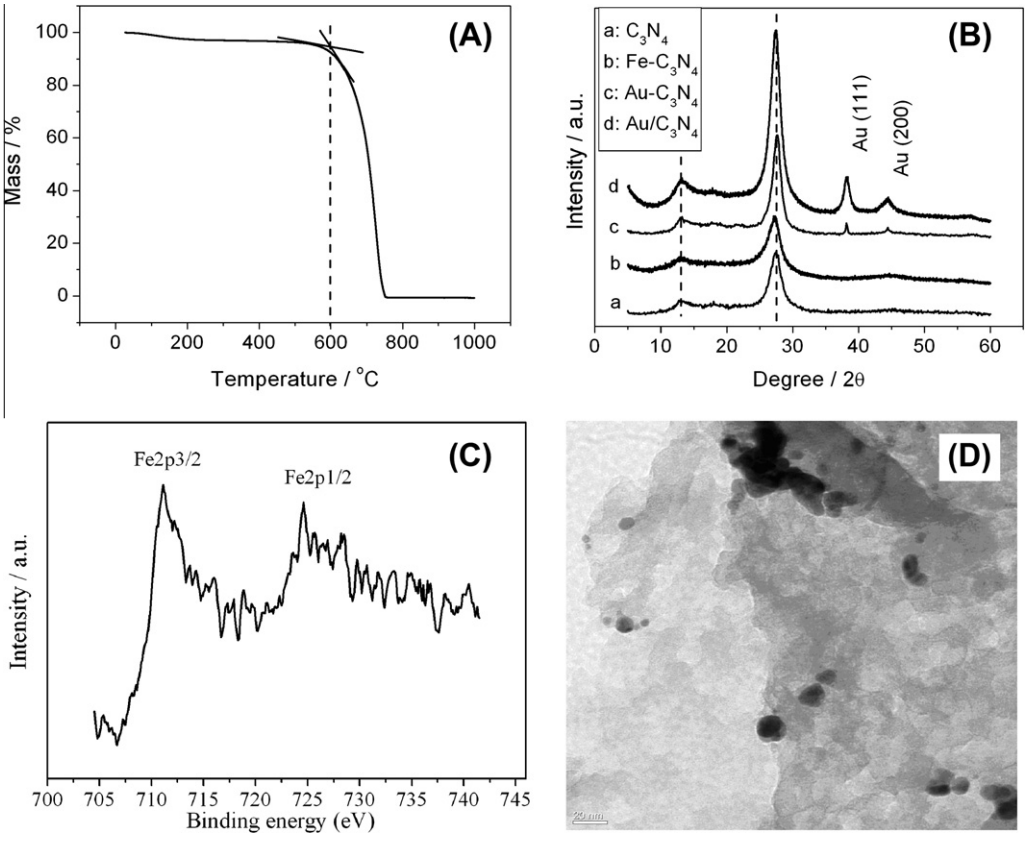

Fig. 1. Some characterization results of the investigated samples: (A) TGA curve of pure C_3N_4; (B) XRD patterns of the catalysts ("Au–C_3N_4" means that the gold catalyst was in situ synthesized; "Au/C_3N_4" means that the gold catalyst was prepared by the immobilization method); (C) XPS spectrum of Fe–C_3N_4 (adapted from Ref. [47]); (D) TEM images of Au/C_3N_4.

$FeCl_3$ added (~10 wt.% Fe–C_3N_4). The solution was continually heated at 80 °C to evaporate water. The resulting reddish mixture was heated at 2 °C/min to 600 °C and maintained there for 4 h under flow nitrogen (99.99%, 100 mL/min), followed by naturally cooling to room temperature under the same atmosphere.

Synthesis of Au–C_3N_4: Cyanamide of 9.8 g was first dissolved in 20 mL deionized water with stirring and 1–3 mL 0.01522 M $HAuCl_4$ solution was added. The mixture was heated up to 90 °C until all the water was evaporated. The obtained white solid was dried at 110 °C for 5 h and heated at 2 °C/min to 550 °C in static air and maintained there for 4 h.

Synthesis of Au/C_3N_4: Mesoporous C_3N_4 was synthesized according to the literature [48]. Then, the "gold colloidal" method [10] was used to prepare the Au/C_3N_4 catalyst. The procedure is similar to that used for Au/AC described below in detail.

Modification of the carbon support: Activated Carbon Aerosorb LR4 from Degussa was first treated in 5% O_2/N_2 (20 mL/min) at 400 °C for 10 h (hereafter denoted as AC5), and subsequently heated at 1 °C/min in inert atmosphere (20 mL/min) to 650, 735, 820, and 910 °C, and maintained there for 1 h. The obtained carbon supports were, accordingly, denoted as AC5_T (with T = 650, 735, 820 and 910, respectively).

Synthesis of Au/AC: Gold catalysts supported on activated carbon (loading: 1wt. %) were prepared by the "gold colloidal" method, similar to that reported by Onal et al. [49]. Briefly, 1 mL of $HAuCl_4$ solution (0.02 g Au per mL) and 1.6 mL of PVA solution (1 wt%) were poured into 250 mL of water, and ca. 5 min. later, 4 mL of fresh $NaBH_4$ solution (0.1 M) was slowly added. The gold sol was formed immediately. After that (~10 min.), 2 g activated carbon was added to the mixture for gold immobilization. The whole process lasted about 3–4 h with strong stirring. The adsorbed support was then filtered and washed with water (the filtrated water was clear for all samples, indicating that gold was completely deposited on the support) until the filtrate was chloride-free ($AgNO_3$ was used for testing) and dried at 110 °C overnight. The dry catalyst was treated in flowing N_2 (40 mL/min) at 350 °C (heating rate of 1 °C/min.) for 3 h, in order to remove the organic scaffold, and immediately activated in flowing H_2 (40 mL/min) at 350 °C for 3 h. The obtained gold catalysts were named according to the original carbon supports as Cat5 and Cat5_T (T = 650, 735, 820 and 910).

2.2. Characterization

TGA of C_3N_4 was carried out on a PerkinElmer STA 6000 in oxygen atmosphere (20 mL/min) with a heating rate of 10 °C/min.

XRD patterns were performed on a Bruker D8 Advance diffractometer with Cu Kα radiation (λ = 0.154 nm) at room temperature (25 °C). The scan step was 0.1° and the step time 1 s.

XPS spectra were recorded on a VG ESXALB MK-II XPS system with a monochromatized Mg Ka X-ray source (35 W). All binding energies were referenced to the C 1s peak at 288.2 eV, which corresponds to the C–N–C coordination in C_3N_4 [47].

TEM images were performed on a Philips CM12 instrument (120 keV), using carbon-coated copper grids (the specimens were loaded directly on the copper grids; no solvent dispersion was used).

TPD profiles of CO and CO_2 were obtained in a fully automated AMI-200 Catalyst Characterization Instrument (Altamira Instruments). In a typical TPR experiment, ~50 mg of sample was placed in a U-shaped quartz tube located inside an electrical furnace and subjected to a 5 °C/min heating rate up to 1100 °C, under a He flow of 25 cm^3/min. The amounts of CO and CO_2 desorbed from the carbon samples were monitored with a quadrupole mass spectrometer.

2.3. Catalytic reaction

Oxidation of CO: The reaction was performed in a continuous-flow reactor as described in a previous work [50]. The powder catalyst (200 mg, <80 mesh) was placed on a quartz (silica) wool bed in a silica tube, which was inserted into a vertical furnace equipped with a temperature controller. Reactant gases (5% CO, 10% O_2 in Helium, 50 mL/min) were dried by passing through silica gel and 4 Å molecular sieves before flowing through the catalytic bed. The composition of the outgoing gas stream was determined at the exit of the tube using a GC equipped with a thermal conductivity detector (TCD). The CO conversion was calculated with the following equation: % CO conversion = $\{[CO]_{in} - [CO]_{out}\}/[CO]_{in} \times 100$, where $[CO]_{in}$ and $[CO]_{out}$ are the initial and end CO concentrations.

Oxidation of benzyl alcohol: The reaction was carried out at atmospheric pressure, in a 50-ml, three-necked batch reactor fitted with a reflux condenser, oil bath, thermocouple, and magnetic stirrer. Typical reaction conditions were the following: 20 ml toluene, 40 μl NaOH (5 M), 20 μl benzyl alcohol, 10 μl decane (internal standard), 0.05 g catalysts (<80 mesh), oxygen (99.99%) flow rate: 50 mL/min, reaction temperature: 80 °C and reaction time: 3 h. The products were analyzed by GC (DANI 1000) with a flame ionization detector, using a CP-Sil 8 CB column and N_2 as carrier gas. The catalytic activity was calculated by the way as indicated in our previous work [11].

3. Results and discussion

The new matrix (C_3N_4) used in this work plays a crucial role in clarifying the mechanism of oxygen activation. Covalently polymeric carbon nitride (C_3N_4) has several allotropes, and the graphitic one (g-C_3N_4) is considered to be the most stable in ambient conditions. The g-C_3N_4 allotrope has a tri-*s*-triazine-based framework, and it can be synthesized simply by thermal condensation of cyanamide or dicyandiamide at 550 °C for 4 h in air atmosphere [48,51]. Elemental analysis and XPS measurements show that g-C_3N_4 consists of carbon, nitrogen, and a small amount of hydrogen (~1.54% wt., according to the C:N:H molar ratio obtained by elemental analysis, which is 3:4.5:1.5), no oxygen being involved [47,52], indicating that g-C_3N_4 is inert to oxygen even at temperature as high as 550 °C. This is confirmed by the TGA experiment shown in Fig. 1A. Thus, it could be an adequate material in order to clarify the pathway of oxygen activation in catalytic oxidation. For example, if the catalyst "M + C_3N_4" ("M" = metal) shows no activity in the oxidation reaction, then it may be inferred that "M" is ineffective for oxygen activation.

Two non-oxygen-containing catalysts, Fe–C_3N_4 (~10 wt.% Fe) and Au/C_3N_4 (~1 wt.% Au) were synthesized as described in the experimental section. Sample Au/C_3N_4 was prepared by a conventional "colloidal gold" method [10], while sample Fe–C_3N_4 was synthesized in situ [47], since it is not possible to deposit Fe^{3+} ions on a C_3N_4 support (i.e., to produce Fe/C_3N_4) without introducing oxygen by a conventional method. XRD results shown in Fig. 1B indicate that no diffraction peak that can be assigned to Fe oxides (e.g. FeO, Fe_2O_3) was observed in Fe–C_3N_4, confirming the successful synthesis of a sample without oxygen. To detect the oxidation state of Fe in Fe–C_3N_4, XPS measurements were carried out and are shown in Fig. 1C, indicating that Fe is not in the metallic state (Fe^0) in Fe–C_3N_4, but still in the Fe^{3+} oxidation state [47]. This allows for comparison with oxide catalysts, like Fe^{3+} in Fe_2O_3. According to the results reported by Wang et al. [47], the Fe^{3+} ions entered into the matrix structure of C_3N_4 and formed a metal–organic hybrid material (i.e. Fe–C_3N_4). The surface Cl/Fe molar ratio determined for this catalyst by the XPS spectra was 0.21 [47],

which is much lower than the ratio of 3:1 present in the starting $FeCl_3$ precursor, indicating that only a minor amount of chloride remains in the sample. As for the gold catalyst, diffraction peaks that indexed both to C_3N_4 and to Au were observed. A comparison of the gold diffraction peaks with those reported in the literature [53] suggests the formation of Au crystals in Au/C_3N_4. The gold particle size evaluated by the Scherrer equation (i.e. $D = k\lambda/\beta\cos\theta$, where $k = 0.89$, $\lambda = 0.154056$ nm, $\beta = 1.39\pi/180$, $\theta = 13.8°$) is ~8.4 nm, which is similar to that determined by TEM (d = ~8.8 nm, see Fig. 1D), showing that these gold particles, if deposited on an oxide support (e.g. Al_2O_3), should be active for CO oxidation [54].

Fig. 2 displays the catalytic behavior of samples in CO oxidation. Very low activities are observed for Fe–C_3N_4 at $T \leqslant 300$ °C and for Au/C_3N_4 up to 500 °C. It has been largely reported, however, that metal oxides (such as Fe_2O_3) and supported gold (e.g. Au/Fe_2O_3) catalysts can show very high activity (~100%) for CO oxidation even at $T < 300$ °C [55,56]. Thus, the low activity observed here indicates that the metal sites of the catalyst are ineffective for oxygen activation and that Au nanoparticles up to 500 °C are also ineffective, since the C_3N_4 support is inert to oxygen. One might argue that the low activity could also be the reason why CO was not activated, but this can be excluded since gaseous CO is also reactive toward activated oxygen (a Rideal–Eley mechanism taking place) [15]. Also, the effect of chloride on the activity could be excluded, since the chloride-free catalyst (Au/C_3N_4 prepared by "gold colloidal" method, being the absence of chloride checked by the $AgNO_3$ method [49]) also shows negligible activity for CO oxidation (see Fig. 2). Thus, the low activity observed must be ascribed to the fact that molecular oxygen was not activated. As a result, it could be deduced that the activation of molecular oxygen in gas phase oxidation reactions does not take place on the metal sites of the catalyst, even for supported gold materials. Otherwise, if oxygen activation could proceed on the metal site, activated oxygen would be able to react with the activated/gaseous CO to give high CO conversions, which is obviously not supported by the results shown in Fig. 2.

It was, however, proposed that CO oxidation activity is closely related to the structure of gold catalysts [57–60]. To exclude that the low activity observed here is due to a structure effect, Au–C_3N_4 catalysts were prepared by an "in situ" method (similar to the synthesis of Fe–C_3N_4) and with different gold contents (by adding 1–3 mL of Au precursor). Results in Fig. 2 (insert picture) show that all of them exhibit negligible activity for CO oxidation (5–8% CO conversion at 500 °C). This indicates that, whatever the preparation method used and the amount of gold added (which could lead to different gold structure), the gold containing C_3N_4 catalyst is not able to catalyze CO oxidation. Considering that the C_3N_4 matrix is inert to oxygen and that CO can participate in the reaction either in the gaseous or in the adsorbed state, it can therefore be inferred that the low activity is due to the fact that molecular oxygen is not activated, that is, gold is not able to activate molecular oxygen.

Based on theoretical calculations or experimental evidence, some authors propose that oxygen activation can proceed at the interface between gold particles and the support [20,25,61]. Although this possibility cannot be excluded, the low activity observed suggests that this is not the case in the present study.

In order to explain the behavior observed for sample Fe–C_3N_4 at 300 °C, where an abrupt increase in CO conversion was observed (see Fig. 2), XRD experiments were performed for this material, calcined in air at 300 and 400 °C, as shown in Fig. 3. The C_3N_4 matrix largely disappeared, and diffraction peaks indexed to Fe_2O_3 were found after calcination in air at 400 °C, while no change occurred at 300 °C. Thus, the increase in activity of Fe–C_3N_4 for CO oxidation at $T > 300$ °C, shown in Fig. 2, may be explained by the destruction of the C_3N_4 matrix (a TGA test showed ~60% weight loss after calcination in air at 400 °C) and the formation of Fe_2O_3, which is active for CO oxidation [55,56]. Recalling that Fe^{3+} is not able to activate molecular oxygen, the high activity observed suggests that molecular oxygen must be activated on the defect or lattice oxygen site of Fe_2O_3. This is expected, since a Mars van Krevelen mechanism could be operative in CO oxidation on Fe_2O_3 [3]. Namely, CO first reacts with the lattice oxygen of Fe_2O_3, yielding an oxygen vacancy, which then acts as the site for molecular oxygen adsorption and activation. In other words, the high activity observed at $T > 300$ °C is due to the presence of oxygen in Fe_2O_3, which activates molecular oxygen. However, it should be noted that this behavior does not occur with the Au–C_3N_4 catalyst, which was prepared by calcination in air at 550 °C for 4 h; thus, no change in activity was observed for the gold catalysts in the entire temperature range studied.

Therefore, it can be concluded that either gold or the transition metal ion of the catalyst is not able to activate molecular oxygen in oxidation reactions; and thus, the step of oxygen activation must occur on other sites, such as the defects or oxygen vacancies of the catalyst. The role of the oxygen (vacancies) site on the oxygen activation process, and thus on the activity for CO oxidation, has been discussed in the literature. For example, Fierro et al. [62]

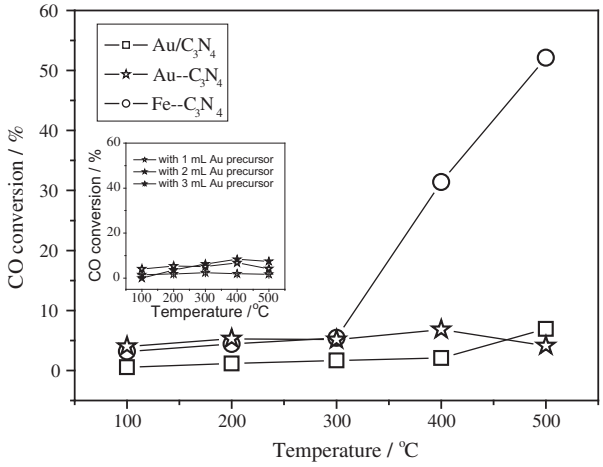

Fig. 2. CO oxidation activity measured with Fe–C_3N_4 and Au–C_3N_4 samples synthesized in situ, and with Au/C_3N_4 prepared by immobilization method, in the temperature range of 100–500 °C; the insert picture shows the CO oxidation activity measured with Au–C_3N_4 samples synthesized in situ with different amounts of Au precursor being added.

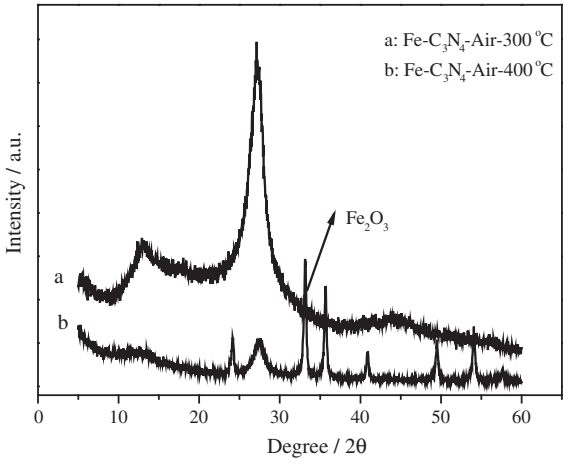

Fig. 3. XRD patterns of the Fe–C_3N_4 catalyst calcined in air at 300 and 400 °C.

investigated the catalytic performance of $LaCuO_{3-\delta}$ for CO oxidation and found that the activity at high temperatures depends on the amount of oxygen vacancies created in the samples. CO oxidation was also investigated on $La_{2-x}Sr_xCuO_{4-\delta}$ [63], similar trends being found. Corma et al. [6] recently investigated CO oxidation on gold catalysts supported on Fe-doped TiO_2 and clearly pointed out that the high activity was due to the presence of defects that activate oxygen. Overall, these results indicate that the oxygen vacancies of the catalyst are the sites for oxygen activation.

Liquid phase selective oxidation using molecular oxygen as the oxidant was also investigated. In these experiments, Fe–C_3N_4 and Au/C_3N_4 catalysts showed negligible activity for oxidation of benzene to phenol or for oxidation of benzyl alcohol to benzaldehyde (conversion <6%), as expected. That is, the metal site of the catalyst is also not able to activate oxygen in the liquid phase oxidation reaction, and the activity observed in oxygen-containing catalysts [11] should be due to the presence of defects or oxygen sites, where oxygen activation occurs.

In order to make a more detailed investigation into the activation process in liquid phase oxidation, a carbon-supported gold catalyst (Au/AC), which is a promising candidate for this type of reaction [10], was used for the selective oxidation of benzyl alcohol to benzaldehyde. One advantage of using carbon as support is that the oxygen content (i.e. the amount of surface oxygen functional groups of the carbon support) can be easily controlled by thermal treatment under inert atmosphere (e.g. N_2) at different temperatures [41].

It should be pointed out that gas phase oxidation of carbon materials changes both their texture and surface chemistry, while thermal treatments under inert atmosphere do not produce significant textural changes with respect to the parent materials [41]. Therefore, the carbon support used in this work was first treated in 5% O_2/N_2 and then thermally treated in N_2 atmosphere at different temperatures. Thus, the influence of textural changes on catalyst activity could be neglected, and only the influence of surface chemistry (e.g. the amounts of surface oxygen functional groups) needs to be taken into account.

Fig. 4A and B shows the TPD profiles of the carbon supports treated in N_2 at different temperatures. Obviously, the amounts of CO and CO_2 released from the carbon supports decrease as the treatment temperature increases, in the sequence of AC5 > AC5_650 > AC5_735 > AC5_820 > AC5_910, indicating the decrease in surface groups. Detailed CO and CO_2 data are listed in Table 1. The small amounts of CO_2 released by some samples below 400 °C are due to re-oxidation, when the samples were exposed to the atmosphere. Besides, in order to check if the catalysts would have the same trend as the supports, that is, the sequence of surface groups would not change after the preparation process, TPD experiments of two catalysts, Cat5 and Cat5_910, were carried out. Results in Fig. 4C and D clearly show that the amount of surface groups of sample Cat5 is much larger than that of Cat5_910, indicating a similar trend as that observed for the carbon support.

Fig. 5 shows the results of the conversion of benzyl alcohol over a series of Au/AC catalysts, in which the carbon support was thermally treated in N_2 at different temperatures. For example, Cat5_650 means that the carbon support was first treated in 5% O_2/N_2 (i.e. AC5), followed by a thermal treatment in N_2 at 650 °C (AC5_650), then the gold particles were deposited on the support AC5_650 to obtain catalyst Cat5_650. The conversion decreased as the treatment temperature of the carbon support increased, that is, Cat5 > Cat5_735 > Cat5_820 > Cat5_910, which is in the same sequence as the amount of surface oxygen functional groups of carbon support (see Fig. 4 and Table 1). This suggests that the amount of oxygen-containing species has a strong effect on the reaction.

It is known that the adsorption and activation of the substrate takes place on the gold site [11,18,64,65], thus the activity pattern observed must be related to the steps of oxygen adsorption and activation. It should be mentioned that, although the gold particle

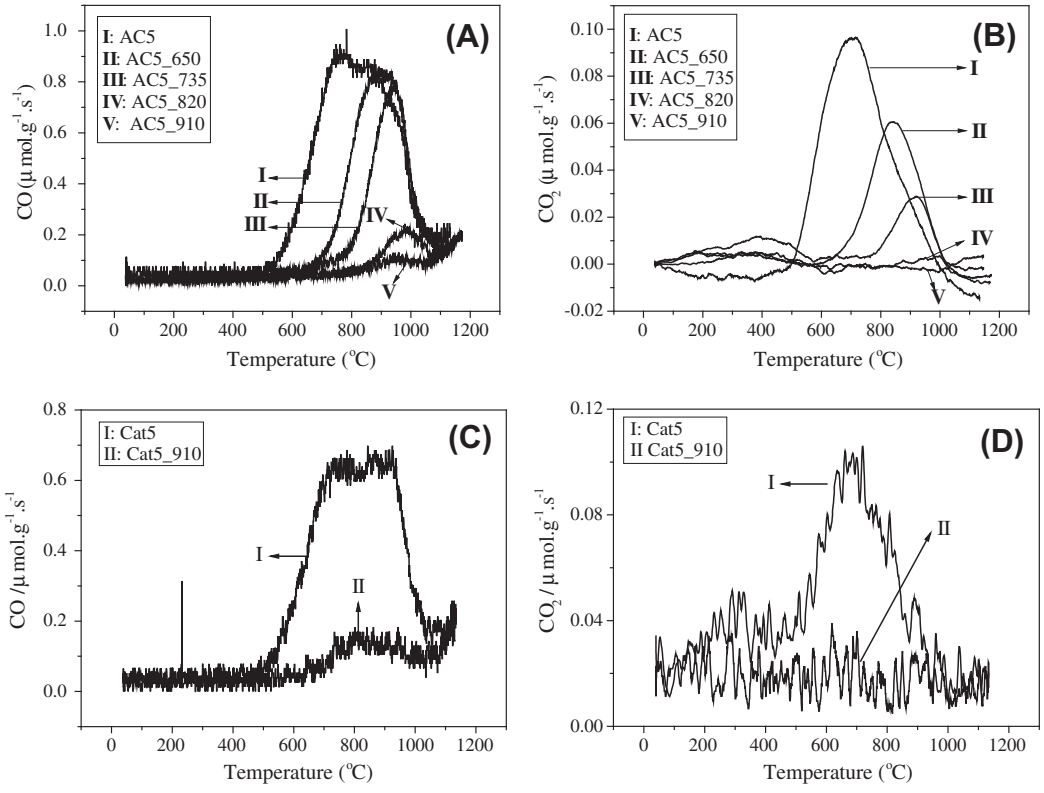

Fig. 4. (A) and (B): TPD of CO and CO_2 obtained from the carbon supports; (C) and (D): TPD of CO and CO_2 obtained from two selected catalysts (Cat5 and Cat5_910).

Table 1
Amounts of CO and CO_2 released from the carbon supports AC5 and AC5_T.

Samples	CO_2 (μmol/g)	CO (μmol/g)
AC5	29	248
AC5_650	13	157
AC5_735	4.6	98
AC5_820	–	14
AC5_910	–	5.6

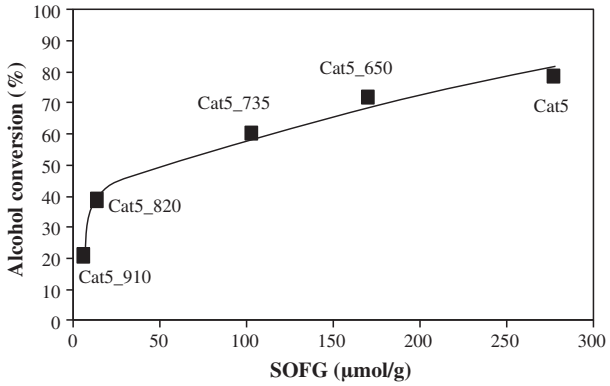

Fig. 5. Conversion of benzyl alcohol obtained with the catalysts Cat5_T, *versus* the amount of surface oxygen functional groups (SOFG) of the corresponding carbon supports (AC5_T).

size of Cat5_910 ($d_{aver.}$ = ~6.4 nm) is a little larger than that of Cat5 ($d_{aver.}$ = ~5.6 nm, see Fig. 6), this impact could be neglected. Actually, it was reported that the optimum gold particle size of Au/AC catalyst for liquid phase oxidation is at ~7.5 nm [66], which means that Cat5_910 should be more active for this reaction. Therefore, the decreasing activity observed in Fig. 5 should not be ascribed to the different gold particle sizes of the samples. Considering that the major difference in the materials is the amount of surface oxygen functional groups, it can be concluded that adsorption and activation of molecular oxygen indeed takes place on these surface groups. That is, the oxygenated surface groups of the activated carbon are responsible for the activation of molecular oxygen. This is in agreement with the results reported by Pigamo et al. [67], who suggested that in liquid phase oxidation reaction, AC can exhibit strong interaction with oxygen through the surface groups: e.g. (1) molecular oxygen can be activated on the surface groups of carbon; (2) oxygen consumed from the surface groups can be continuously regenerated during the reaction.

To further confirm that the gold particles are not able to activate molecular oxygen, a leaching experiment was carried out, using a similar process as described by Sheldon et al. [68]: after the reaction proceeded for 1 h, the catalyst was filtered, and the reaction was left to continue for another 1 h. The conversions determined before and after filtering were ~64% and ~65%, respectively, indicating that the reaction is heterogeneous. That is, the leached gold cannot activate molecular oxygen. This is in accordance with the results reported in the literature, such as those of Suib and coworkers [9] and Baiker and coworkers [69], which concluded that leaching of the active species (i.e. Mn or Ru) does not lead to homogeneous catalysis in the aerobic oxidation of alcohols.

However, it is known that the presence of basicity (e.g. NaOH) is essential for gold catalyzed liquid phase alcohol oxidation by molecular oxygen [11,65,70,71]. A detailed investigation, previously carried out [11], showed that the role of basicity is not to activate molecular oxygen, but to promote the adsorption and

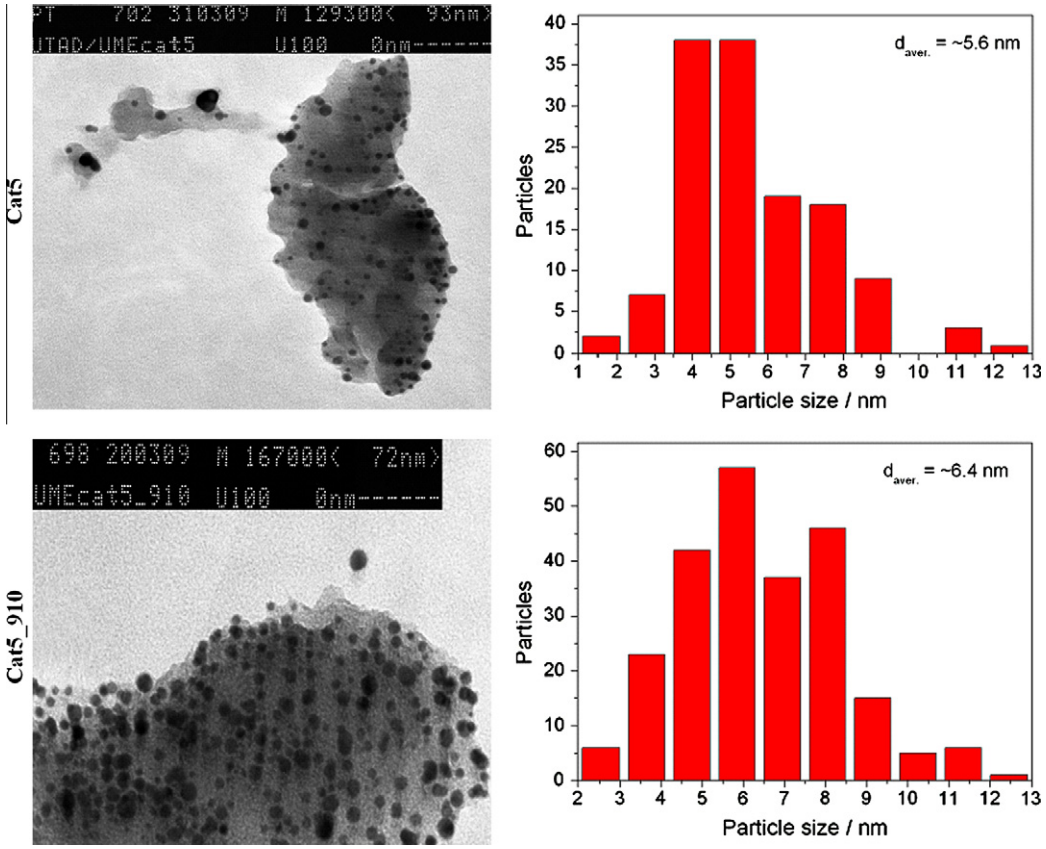

Fig. 6. TEM images and the corresponding gold particle size distributions of Cat5 and Cat5_910.

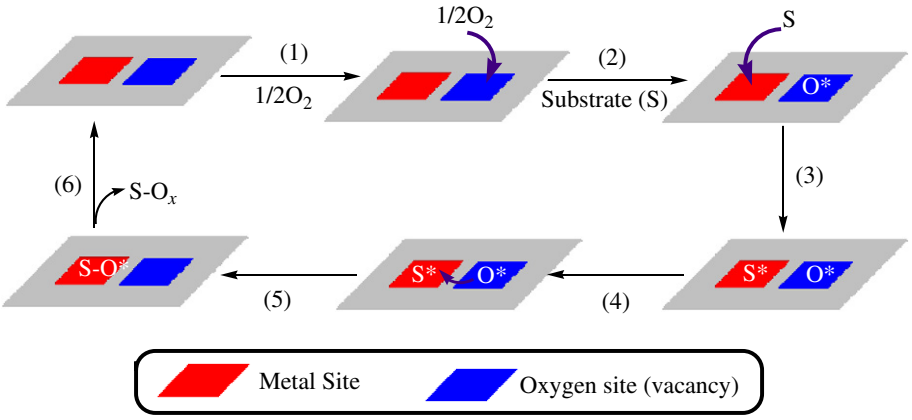

In step (2) only one atom of oxygen is shown for simplicity; the amount of atomic oxygen consumed in the reaction is represented by "x" in step (6)

Scheme 1. Proposed mechanism for the activation of substrate and oxygen in the oxidation reaction.

activation of the substrate on the gold surface (as shown below in reactions (1)–(4)). Therefore, it is proposed that the activation of oxygen on Au/AC catalysts indeed occurs through the surface oxygen functional groups of the carbon support:

$$Au/AC + (OH^-)_{bulk} \rightleftarrows [Au{-}OH^-]/AC \quad (1)$$

$$(PhCH_2OH)_{bulk} + [Au{-}OH^-]/AC \rightleftarrows [PhCH_2OH{-}Au{-}OH^-]/AC \quad (2)$$

$$[PhCH_2OH{-}Au{-}OH^-]/AC + O_2 \rightarrow [PhCHO{-}Au]/AC + H_2O + (OH^-)_{bulk} \quad (3)$$

$$[PhCHO{-}Au]/AC \rightleftarrows (PhCHO)_{bulk} + Au/AC \quad (4)$$

4. Conclusions

The following conclusions can be drawn from the results presented earlier:

1. Catalysts without oxygen have negligible activity for CO oxidation, as observed with Fe–C_3N_4 and Au/C_3N_4 catalysts at $T < 300$ °C (see Fig. 2).
2. The oxidation activity increased abruptly when oxygen was present on the catalyst, as observed with "Fe–C_3N_4" at $T > 300$ °C, when Fe_2O_3 oxide was present, as illustrated in Figs. 2 and 3.
3. As a result of 1 and 2, it can be inferred that gold or transition metal alone is not able to activate molecular oxygen; therefore, oxygen activation must proceed on the other sites of the catalyst, such as defects or oxygen vacancies.
4. For liquid phase oxidation reactions with molecular oxygen as oxidant, the conversion of substrate closely depends on the amount of oxygen species of the catalyst. The activity of Au/AC for benzyl alcohol oxidation followed the order: Cat5 > Cat5_735 > Cat5_820 > Cat5_910, which is in the same sequence as the amount of surface oxygen functional groups of the carbon supports, as shown in Fig. 5.

Therefore, adsorption and activation of oxygen in oxidation reactions occur on the defects or oxygen vacancies of the catalyst, while that of the substrate takes place on the metal sites of the catalyst, as illustrated in Scheme 1.

Acknowledgments

J. Zhu thanks Prof. X. Wang in Max-Planck Institute of Colloids and Interfaces and Prof. A. Thomas in Technical University of Berlin for help in preparation and discussions on the C_3N_4 and Fe–C_3N_4 materials. This work was partially financed by German Research Foundation (DFG, Grant No. TH 1463/5-1), Fundação para a Ciência e a Tecnologia (FCT) with contribution from FEDER (Projects POCTI/EQU/58252/2004 and PTDC/EQU-ERQ/101456/2008). Additional support was provided from FCT to SAC (CIENCIA 2007 program) and to JZ (SFRH/BPD/28390/2006).

References

[1] V.D. Sokolovskii, Catal. Rev. 32 (1990) 1.
[2] Y. Ren, Z. Ma, L.P. Qian, S. Dai, H.Y. He, P.G. Bruce, Catal. Lett. 131 (2009) 146.
[3] A.K. Kandalam, B. Chatterjee, S.N. Khanna, B.K. Rao, P. Jena, B.V. Reddy, Surf. Sci. 601 (2007) 4873.
[4] G.J. Hutchings, M.S. Hall, A.F. Carley, P. Landon, B.E. Solsona, C.J. Kiely, A. Herzing, M. Makkee, J.A. Moulijn, A. Overweg, J.C. Fierro-Gonzalez, J. Guzman, B.C. Gates, J. Catal. 242 (2006) 71.
[5] S.T. Daniells, A.R. Overweg, M. Makkee, J.A. Moulijn, J. Catal. 230 (2005) 52.
[6] S. Carrettin, Y. Hao, V. Aguilar-Guerrero, B.C. Gates, S. Trasobares, J.J. Calvino, A. Corma, Chem. – Eur. J. 13 (2007) 7771.
[7] M. Comotti, W.C. Li, B. Spliethoff, F. Schuth, J. Am. Chem. Soc. 128 (2006) 917.
[8] V.D. Makwana, Y.C. Son, A.R. Howell, S.L. Suib, J. Catal. 210 (2002) 46.
[9] Y.C. Son, V.D. Makwana, A.R. Howell, S.L. Suib, Angew. Chem. Int. Ed. 40 (2001) 4280.
[10] L. Prati, G. Martra, Gold. Bull. 32 (1999) 96.
[11] J.J. Zhu, J.L. Figueiredo, J.L. Faria, Catal. Commun. 9 (2008) 2395.
[12] R.G. Quiller, X.Y. Liu, C.M. Friend, Chem. – Asian J. 5 (2010) 78.
[13] R.D. Wragg, P.G. Ashmore, J.A. Hockey, J. Catal. 28 (1973) 337.
[14] F. Boccuzzi, A. Chiorino, S. Tsubota, M. Haruta, J. Phys. Chem. 100 (1996) 3625.
[15] Y. Zhang-Steenwinkel, L.M. van der Zande, H.L. Castricum, A. Bliek, Appl. Catal. B – Environ. 54 (2004) 93.
[16] G.W. Keulks, J. Catal. 19 (1970) 232.
[17] H.H. Kung, M.C. Kung, C.K. Costello, J. Catal. 216 (2003) 425.
[18] T. Ishida, M. Nagaoka, T. Akita, M. Haruta, Chem. – Eur. J. 14 (2008) 8456.
[19] G.C. Bond, D.T. Thompson, Gold Bull. 33 (2000) 41.
[20] M.M. Schubert, S. Hackenberg, A.C. van Veen, M. Muhler, V. Plzak, R.J. Behm, J. Catal. 197 (2001) 113.
[21] Z. Yan, S. Chinta, A.A. Mohamed, J.P. Fackler, D.W. Goodman, J. Am. Chem. Soc. 127 (2005) 1604.
[22] M. Haruta, M. Date, Appl. Catal. A – Gen. 222 (2001) 427.
[23] H. Liu, A.I. Kozlov, A.P. Kozlova, T. Shido, K. Asakura, Y. Iwasawa, J. Catal. 185 (1999) 252.
[24] M. Okumura, J.M. Coronado, J. Soria, M. Haruta, J.C. Conesa, J. Catal. 203 (2001) 168.
[25] Z.P. Liu, X.Q. Gong, J. Kohanoff, C. Sanchez, P. Hu, Phys. Rev. Lett. 91 (2003) 266102.
[26] M. Haruta, Nature 437 (2005) 1098.
[27] Y. Iizuka, H. Fujiki, N. Yamauchi, T. Chijiiwa, S. Arai, S. Tsubota, M. Haruta, Catal. Today 36 (1997) 115.
[28] Y. Iizuka, T. Tode, T. Takao, K. Yatsu, T. Takeuchi, S. Tsubota, M. Haruta, J. Catal. 187 (1999) 50.
[29] Y. Iizuka, A. Kawamoto, K. Akita, M. Date, S. Tsubota, M. Okumura, M. Haruta, Catal. Lett. 97 (2004) 203.
[30] V. Zielasek, B. Jurgens, C. Schulz, J. Biener, M.M. Biener, A.V. Hamza, M. Baumer, Angew. Chem. Int. Ed. 45 (2006) 8241.

[31] E. Quinet, L. Piccolo, H. Daly, F.C. Meunier, F. Morfin, A. Valcarcel, F. Diehl, P. Avenier, V. Caps, J.L. Rousset, Catal. Today 138 (2008) 43.
[32] S.A.C. Carabineiro, B.E. Nieuwenhuys, Gold Bull., in press.
[33] J.M. Gottfried, K. Christmann, Surf. Sci. 566 (2004) 1112.
[34] B.K. Min, A.R. Alemozafar, D. Pinnaduwage, X. Deng, C.M. Friend, J. Phys. Chem. B 110 (2006) 19833.
[35] S. Al-Sayari, A.F. Carley, S.H. Taylor, G.J. Hutchings, Top. Catal. 44 (2007) 123.
[36] J.L. Gong, C.B. Mullins, Accounts Chem. Res. 42 (2009) 1063.
[37] J. Biener, M.M. Biener, T. Nowitzki, A.V. Hamza, C.M. Friend, V. Zielasek, M. Baumer, ChemPhysChem 7 (2006) 1906.
[38] E. Samano, J. Kim, B.E. Koel, Catal. Lett. 128 (2009) 263.
[39] J.L.C. Fajin, M.N.D.S. Cordeiro, J.R.B. Gomes, J. Phys. Chem. C 112 (2008) 17291.
[40] J.A. Rodriguez, L. Feria, T. Jirsak, Y. Takahashi, K. Nakamura, F. Illas, J. Am. Chem. Soc. 132 (2010) 3177.
[41] J.L. Figueiredo, M.F.R. Pereira, M.M.A. Freitas, J.J.M. Orfao, Carbon 37 (1999) 1379.
[42] J.L. Figueiredo, M.F.R. Pereira, M.M.A. Freitas, J.J.M. Orfao, Ind. Eng. Chem. Res. 46 (2007) 4110.
[43] N.M. Gupta, A.K. Tripathi, J. Catal. 187 (1999) 343.
[44] A.K. Tripathi, V.S. Kamble, N.M. Gupta, J. Catal. 187 (1999) 332.
[45] H.C. Liu, A.I. Kozlov, A.P. Kozlova, T. Shido, Y. Iwasawa, Phys. Chem. Chem. Phys. 1 (1999) 2851.
[46] Y. Wu, T. Yu, B.S. Dou, C.X. Wang, X.F. Xie, Z.L. Yu, S.R. Fan, Z.R. Fan, L.C. Wang, J. Catal. 120 (1989) 88.
[47] X.C. Wang, X.F. Chen, A. Thomas, X.Z. Fu, M. Antonietti, Adv. Mater. 21 (2009) 1609.
[48] X.C. Wang, K. Maeda, X.F. Chen, K. Takanabe, K. Domen, Y.D. Hou, X.Z. Fu, M. Antonietti, J. Am. Chem. Soc. 131 (2009) 1680.
[49] Y. Onal, S. Schimpf, P. Claus, J. Catal. 223 (2004) 122.
[50] S.A.C. Carabineiro, B.F. Machado, R.R. Bacsa, P. Serp, G. Drazic, J.L. Faria, J.L. Figueiredo, J. Catal. 273 (2010) 191.
[51] X.C. Wang, K. Maeda, A. Thomas, K. Takanabe, G. Xin, J.M. Carlsson, K. Domen, M. Antonietti, Nature Mater. 8 (2009) 76.
[52] A. Thomas, A. Fischer, F. Goettmann, M. Antonietti, J.O. Muller, R. Schlogl, J.M. Carlsson, J. Mater. Chem. 18 (2008) 4893.
[53] X.P. Sun, S.J. Dong, E.K. Wang, Chem. Commun. (2004) 1182.
[54] S. Ivanova, C. Petit, V. Pitchon, Gold Bull. 39 (2006) 3.
[55] G. Smit, S. Zrncevic, K. Lazar, J. Mol. Catal. A – Chem. 252 (2006) 103.
[56] Y.H. Zheng, Y. Cheng, Y.S. Wang, F. Bao, L.H. Zhou, X.F. Wei, Y.Y. Zhang, Q. Zheng, J. Phys. Chem. B 110 (2006) 3093.
[57] M. Chen, Y. Cai, Z. Yan, D.W. Goodman, J. Am. Chem. Soc. 128 (2006) 6341.
[58] M.S. Chen, D.W. Goodman, Science 306 (2004) 252.
[59] M.S. Chen, D.W. Goodman, Accounts Chem. Res. 39 (2006) 739.
[60] A.A. Herzing, C.J. Kiely, A.F. Carley, P. Landon, G.J. Hutchings, Science 321 (2008) 1331.
[61] L.M. Molina, B. Hammer, Phys. Rev. Lett. 90 (2003) 206102.
[62] H. Falcon, M.J. Martinez-Lope, J.A. Alonso, J.L.G. Fierro, Appl. Catal. B – Environ. 26 (2000) 131.
[63] J.J. Zhu, Z. Zhao, D.H. Xiao, J. Li, X.G. Yang, Y. Wu, Z. Phys. Chem. 219 (2005) 807.
[64] G.C. Bond, D.T. Thompson, Catal. Rev. 41 (1999) 319.
[65] T. Mallat, A. Baiker, Chem. Rev. 104 (2004) 3037.
[66] F. Porta, L. Prati, M. Rossi, S. Coluccia, G. Martra, Catal. Today 61 (2000) 165.
[67] A. Pigamo, M. Besson, B. Blanc, P. Gallezot, A. Blackburn, O. Kozynchenko, S. Tennison, E. Crezee, F. Kapteijn, Carbon 40 (2002) 1267.
[68] R.A. Sheldon, M. Wallau, I.W.C.E. Arends, U. Schuchardt, Accounts Chem. Res. 31 (1998) 485.
[69] Z. Opre, D. Ferri, F. Krumeich, T. Mallat, A. Baiker, J. Catal. 241 (2006) 287.
[70] S. Carrettin, P. McMorn, P. Johnston, K. Griffin, C.J. Kiely, G.J. Hutchings, Phys. Chem. Chem. Phys. 5 (2003) 1329.
[71] S. Biella, L. Prati, M. Rossi, Inorg. Chim. Acta 349 (2003) 253.